Performance Prediction of Switched Reluctance Motor using Improved Generalized Regression Neural Networks for Design Optimization

Zhu Zhang, *Member, IEEE*, Shenghua Rao, and Xiaoping Zhang

***Abstract*—Since practical mathematical model for the design optimization of switched reluctance motor (SRM) is difficult to derive because of the strong nonlinearity, precise prediction of electromagnetic characteristics is of great importance during the optimization procedure. In this paper, an improved generalized regression neural network (GRNN) optimized by fruit fly optimization algorithm (FOA) is proposed for the modeling of SRM that represent the relationship of torque ripple and efficiency with the optimization variables, stator pole arc, rotor pole arc and rotor yoke height. Finite element parametric analysis technology is used to obtain the sample data for GRNN training and verification. Comprehensive comparisons and analysis among back propagation neural network (BPNN), radial basis function neural network (RBFNN), extreme learning machine (ELM) and GRNN is made to test the effectiveness and superiority of FOA-GRNN.**

***Index Terms*—Fruit fly optimization algorithm, generalized regression neural networks, switched reluctance motor.**

I. Introduction

SWITCHED reluctance motor (SRM) is considered as an attractive candidate to high performance applications for its robust structure, high reliability and fast dynamic response. However, relatively high torque ripple and resultant acoustic noise restrict its application field, such as electric vehicle drive system and some servo systems. Moreover, operation efficiency is another crucial index for motion control system. Therefore, there is a continuous need for design optimization of SRM to satisfy specific applications.

Accurate prediction of motor performance is very important during design optimization procedure, but the inherent nonlinearity of SRM makes it very difficult to obtain a practical mathematics model. In order to improve the approximation accuracy of nonlinear characteristics, researchers have been exploring effective solutions for decades, such as magnetic equivalent circuit (MEC), finite element method (FEM), neural networks and fuzzy inference system [1-3].

Fruit fly optimization algorithm (FOA) was proposed by Pan in 2011 [4]. It is a novel population-based intelligence algorithm derived from the foraging process of fruit fly swarm [5]. Compared with other optimization algorithms, FOA has the advantages of relatively simple concept, less adjustable parameters, and efficient calculation process [6-7]. It has been successfully applied in many fields, such as PID controller adjustment [8], neural network training [9] and synchronous generator parameter identification [10], knapsack problem [11], and replenishment problems [12].

This paper proposes a new modeling method of SRM based on improved generalized regression neural networks (GRNN), whose spread parameter is optimized by fruit fly optimization algorithm. The presented model is used for the prediction of torque ripple and operation efficiency with varied optimization variables, like stator pole arc, rotor pole arc and rotor yoke height. Comprehensive comparisons with BPNN, RBFNN and ELM are made to test the effectiveness of GRNN.

II. GRNN

GRNN, proposed by Specht [13], is a kind of probabilistic neural networks with simple structure and high learning speed. Compared with BPNN, it has good performance on non-linear approximation ability, especially when the number of training sample is relatively small. Moreover, there is only one adjustable parameter, called spread parameter, determines the generalization capability of the GRNN. It makes GRNN a very effective way to predict motor performance during optimization procedure.

The structure of GRNN is shown in Fig.1. It has a radial basis layer and a special linear layer.

The radial basis layer can be expressed as

$$a_{1i} = radbas\left(\left\|LW_{1.1i} - p\right\|b_{1i}\right) \tag{1}$$

where a_{1i} is the ith element of output a_1 , $LW_{1.1i}$ is the weighted vector made of the ith row of $LW_{1.1}$. Each neuron's weighted input is the distance between the input vector and its

Manuscript was submitted for review on 30, August, 2018.

This work was supported in part by the National Natural Science Foundation of China under Grant61503132 and Grant51477047, and the Hunan Provincial Natural Science Foundation of China under Grant2015JJ5029.

Zhu Zhang is with the School of Information and Electrical Engineering, Hunan University of Science and Technology, Hunan, China (e-mail: eezhuzhang@ 126.com).

Shenghua Rao, was with the Resources Exploration Equipment and Safety Technology, Hunan University of Science and Technology, Hunan, China (e-mail: 1014791899@qq.com).

Xiaoping Zhang is with the Resources Exploration Equipment and Safety Technology, Hunan University of Science and Technology, Hunan, China (e-mail:511537178@qq.com).

Digital Object Identifier 10.30941/CESTEMS.2018.00047

weight vector. The Gauss basis function is generally used as the transfer function in the first layer

$$R_i = \exp\left(-\frac{(x-ci)^2}{2\sigma_i^2}\right) \tag{2}$$

where σ_i is the spread parameter.

The second layer is expressed as

$$a_2 = purelin\left(n^2\right) \tag{3}$$

where *purelin* represents linear function.

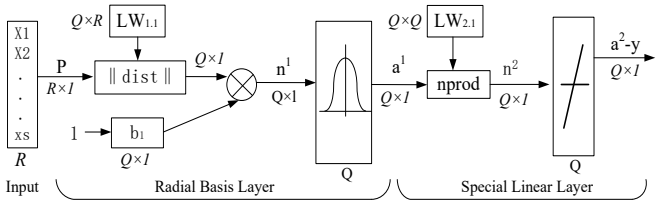

P--Input; Q--Number of input vectors; b1--Implicit layer threshold; $\|\text{dist}\|$--Distance function; R--Number of vector elements per group; $W_{1.1}$--Input layer weight; $LW_{2.1}$--Weight matrix; n2--Output; a2--Linear transfer function; nprod--Normalized dot product;

Fig. 1. The Architecture of GRNN.

III. FOA-GRNN

A. Overview of FOA

FOA is a novel population-based intelligence algorithm derived from the foraging process of fruit fly swarm [4]. Living in tropical and temperate climate zones, fruit flies have a better performance in vision and osphresis than other species. Guided by a special odor, the fruit fly can fly to the location while sending and receiving message from other flies around, and then compare and decide the best location.

The procedure of FOA can be described as follows:

1) Parameters and population initialization

In FOA, the population number NP, the maximum number of iterations T and the random flight distance are the major restrictive factors. In the search space, the flocking position of fruit fly (X_axis, Y_axis) is randomly initialized as it is showed in (4) and (5):

$$X\_axis = LB + rand \times (UB - LB) \tag{4}$$

$$Y\_axis = LB + rand \times (UB - LB) \tag{5}$$

where *rand* plays a random role that generates a value in the interval [0,1] from the uniform distribution; UB and LB represents the upper and lower limit of the flocking location of fruit flies.

2) Osphresis-based search

In this stage, a great number of food sources are generated near the position where fruit flies gather. First of all, the flight direction is obtained at random, and the foraging distance of each fruit fly is given by

$$X_i = X\_axis + rand \quad Value \tag{6}$$

$$Y_i = Y\_axis + rand \quad Value \tag{7}$$

where i = 1, 2, . . . , *NP*, and the function *rand( )* generates a random number between −1 and 1.

Next, the distance between the food and fruit fly (D_i) is calculated, and the judgment value of smell concentration (S_i) is then obtained by (9). As a matter of fact, S_i serves as a candidate solution.

$$D_i = \sqrt{\left(X_i^2 + Y_i^2\right)} \tag{8}$$

$$S_i = 1/D_i \tag{9}$$

Lastly, the smell concentration ($Smell_i$) is calculated by substituting S_i in the fitness function.

$$Smell_i = Fitness\left(S_i\right) \tag{10}$$

3) Vision-based search

A greedy procedure of selection is implemented by FOA in this stage. Firstly, the fruit fly with maximum value of *Smell* is selected from the flock:

$$\left[bestSmell, bestIndex\right] = \max\left(Smell\right) \tag{11}$$

Secondly, the previous maximum smell concentration *Smellbest* is updated with the current value $bestSmell$ if $bestSmell > Smellbest$. As a result, vision leads the fruit flies flocking together at the location with maximum value of smell concentration.

$$Smellbest = bestSmell \tag{12}$$

$$X\_axis = X\left(bestIndex\right) \tag{13}$$

$$Y\_axis = Y\left(bestIndex\right) \tag{14}$$

Only when the smell concentration no longer become larger, or reach the maximum iteration number, will the previous two stages stop repetitive execution.

B. FOA-GRNN

In this paper, FOA is used to obtain the optimal spread parameter of GRNN, with the objective of minimizing average relative error. The optimization procedure of FOA for GRNN is demonstrated in Fig.2. By optimizing the spread parameter, the estimation accuracy can be considerably enhanced. It makes FOA-GRNN a very effective way to predict motor performance during optimization procedure.

The specific optimization steps are as follows:

(1) Randomly give the initial fruit fly population position (*X*, *Y*), and set the number of iterations maxgen and population size;

(2) Randomly set the flight direction of the fruit fly and Distance;

(3) Determine the distance between the individual and the

origin of the fruit fly $D_i^2 = X_i^2 + Y_i^2$ and the taste concentration determination value $S=1/D_i$;

(4) Establish a taste concentration determination function, that is, the fitness function, and substitute the taste concentration determination value S into the fitness function. In order to find the taste concentration of the individual position of the fruit fly, this paper uses the root mean square error of the GRNN prediction model as the taste concentration function, that is, the fitness function;

(5) Finds the extreme value according to the taste concentration value, and compares the taste concentration value of each generation of fruit fly. Iteratively retains the optimal value position and taste concentration, and records the optimal value of each generation;

(6) Fruit fly iterative optimization, repeat steps (2) to (5) to determine whether the taste concentration is better than the previous iteration taste concentration;

(7) Determine whether iteration is reached the number of times required, the optimal spread parameters and the optimal GRNN prediction model are obtained.

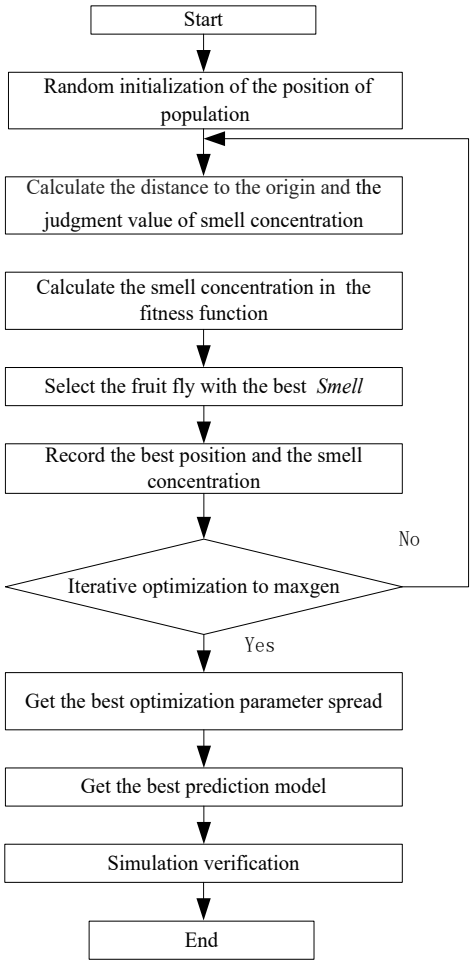

Fig. 2. Optimization procedure of FOA-GRNN.

IV. MODELLING OF SRM

The torque ripple and operating efficiency characteristics of SRM are very sensitive to geometric variables, and there is no pair of stator and rotor pole arcs that meet the criteria of minimum torque ripple and maximum efficiency. The cross-section drawing of SRM with labeled geometric variables is demonstrated in Fig. 3. The specification of considered SRM is listed in Table II.

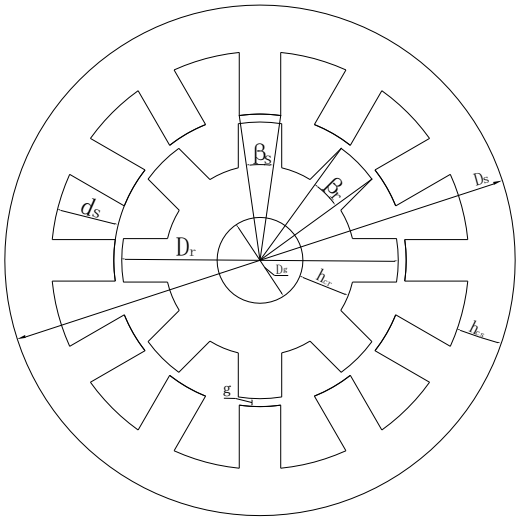

Fig. 3. Cross-section drawing of SRM.

TABLE I
SPECIFICATION OF SRM

Parameters	Value
Rated Power, P_N	4kW
Number of Phase, m	3
Structure	12/8
Rated Speed, n	1500 rpm
Air gap length, g	0.2 mm
Core stack length, l_s	140 mm
Stator Outer diameter, D_s	164 mm
Rotor Outer diameter, D_r	99.8 mm
Rated current, I_N	9 A

In this paper, stator pole arc, rotor pole arc and rotor yoke height are selected as optimization variables. To ensure that SRM has self-starting ability and better static torque characteristic, the selection of stator pole arc and rotor pole arc are constrained in a particular region ABD, called feasible triangle, as shown in Fig.4.

The relationship of the stator and rotor pole arcs、rotor yoke height can be obtained from (15) and (16).

$$\begin{cases} \beta_r + \beta_s \le \dfrac{2\pi}{N_r} \\ \beta_r \ge \beta_s \\ \beta_s \ge \dfrac{2\pi}{mN_r} \end{cases} \tag{15}$$

$$h_{cr} = (1.2 \sim 1.4) \times \frac{b_{pr}}{2} \tag{16}$$

where β_r and β_s are rotor and stator pole arc, respectively. N_r is the number of rotor poles and m is the number of phases.

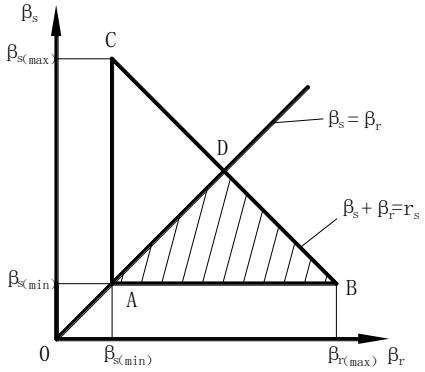

Fig. 4. Feasible Triangle.

The optimization objectives are minimizing torque ripple and maximizing operation efficiency. Hence, FOA-GRNN is used to represent the relationship of torque ripple and efficiency to three variables, as shown in Fig.5. Finite element parametric analysis is carried out to obtain the sample data needed for training and verification of GRNN.

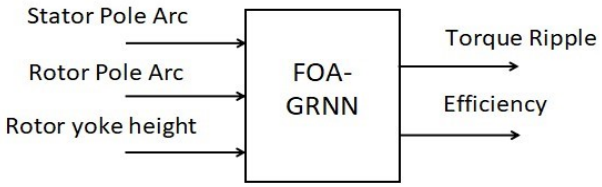

Fig. 5. Modelling of FOA-GRNN

Torque ripple can be evaluated from the torque characteristics $T(i,\theta)$ .The minimum torque $T_{\min}$ occurs at a certain position where equal torque are generated by two overlapping phases at the same level of current. Hence, the torque ripple can be calculated by

$$\delta = \frac{T_{\max} - T_{\min}}{T_{av}} \times 100\% \tag{17}$$

where $T_{\max}$, $T_{\min}$ and T_{av} are the maximum torque, minimum torque and average torque.

The operation efficiency η is given by

$$\eta = \frac{P_o}{P_{IN}} \times 100\% \tag{18}$$

where P_o and P_{IN} are the output power and input power, respectively.

V. Modelling Performance Verification

In order to test the prediction performance of FOA-GRNN, comprehensive comparisons are carried out with BPNN, RBFNN, ELM and standard GRNN.

The relative error *Ei* and coefficient of determination R^2 are selected as criteria to evaluate the performance of the above modelling methods.

$$E_i = \frac{\left|\hat{y}_i - y_i\right|}{y_i} \times 100\%, \quad i = 1,2,\cdots,n \tag{19}$$

$$R^2 = \frac{\left(l\sum_{i=1}^{l}\hat{y}_i y_i - \sum_{i=1}^{l}\hat{y}_i \sum_{i=1}^{l} y_i\right)}{\left(\sum_{i=1}^{l}\hat{y}_i^{\,2} - \left(\sum_{i=1}^{l}\hat{y}_i\right)^2\right)\left(l\sum_{i=1}^{l}\hat{y}_i^{\,2} - \left(\sum_{i=1}^{l} y_i\right)^2\right)} \tag{20}$$

where $\hat{y}_i$ and y_i are the predicted value and actual value, respectively.

Finite element parametric analysis (FEPA) technology is applied to obtain the relationship of torque ripple and efficiency with the optimization variables using Ansoft Maxwell. The values of stator pole arc, rotor pole arc and rotor yoke height are changed individually within the range in accordance with equation (15) and (16). The relationship obtained by FEPA is used as the sample data for training and verification of the above approximation models. 120 sets of sample data are finally selected for each optimization objective.

A. Torque ripple Prediction

Five approximation models are trained with the same 105 sets of sample data obtained by finite element parametric analysis, and another 15 sets of sample data are selected to evaluate the prediction accuracy. The number of input and output node of five models is three and one, respectively.

As the performance of BPNN, RBFNN and ELM has a great relationship with the network structure, the parameters is set based on expert experience and experiments. The key parameters of five models for torque ripple prediction are set as follows. The neuron number in hidden layer of BPNN is 50, the learning rate is 0.01, the learning error is 0.001, and the maximum iteration number is 1000; the expansion speed of RBF is set to 5; the hidden layer node number of ELM is set to 8 and the Sigmoid function is selected as activation function.

The spread parameter of GRNN is optimized by FOA, with the average relative error as the optimization objective. The population size of FOA is 20, and the value is obtained after fifteen iteration. The convergence process is shown in Fig. 6.

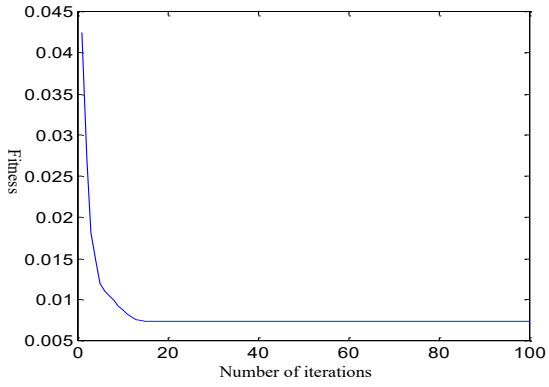

Fig. 6. Convergence process.

The performances of five modeling methods for torque ripple prediction are demonstrated in Fig. 7. The comparison in coefficient of determination and average relative error is illustrated in TABLE II. It is evident that the prediction accuracy of FOA-GRNN outperform other four methods.

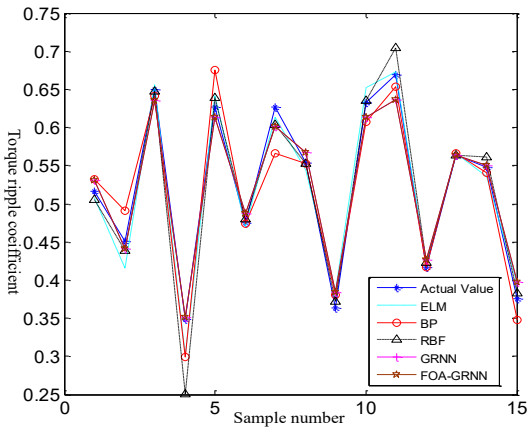

Fig. 7. The performance of torque ripple prediction.

TABLE II
COMPARISON IN TORQUE RIPPLE PREDICTION

	Coefficient of determination	*Average relative error*
BP	0.93274	4.39%
ELM	0.97319	3.28%
RBF	0.95429	3.61%
GRNN	0.98647	2.77%
FOA-GRNN	0.99811	0.74%

B. *Efficiency Prediction*

The key parameters of the above models for efficiency prediction are set as follows. The neuron number in hidden layer of BPNN is 20, the learning rate is 0.01, the learning error is 0.001, and the maximum iteration number is 1000; the expansion speed of RBF is set to 4; the hidden layer node number of ELM is set to 15 and the Sigmoid function is selected as activation function. The population size of FOA is 20, and the spread coefficient is obtained after fourteen iterations. The convergence process is shown in Fig. 8.

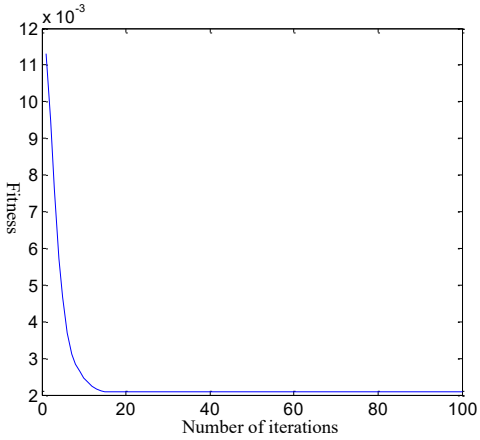

Fig. 8. Convergence process

The performances of five modeling methods for efficiency prediction are demonstrated in Fig.9. The comparison in coefficient of determination and average relative error is illustrated in TABLE III. It is evident that the prediction accuracy of FOA-GRNN is better than other four methods according to the comparison of average relative error and coefficient of determination.

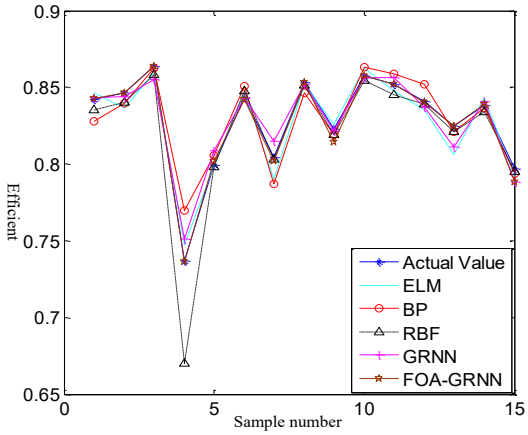

Fig. 9. The performance of efficiency prediction

TABLE III
COMPARISON IN EFFICIENCY PREDICTION

	Coefficient of determination	*Average relative error*
BP	0.86927	1.07%
ELM	0.94269	0.78%
RBF	0.93867	1.01%
GRNN	0.95432	0.68%
FOA-GRNN	0.99210	0.21%

VI. CONCLUSION

In this paper, FOA-GRNN is proposed for the performance prediction of SRM that represent the relationship of torque ripple and efficiency to optimization variables, stator pole arc, rotor pole arc and rotor yoke height. Finite element parametric analysis technology is used to obtain the sample data for training and verification. Comprehensive comparisons and analysis among BP, RBF, ELM and GRNN are carried out that validate the effectiveness and superiority of FOA-GRNN.

REFERENCES

[1] Peng, W., and J. Gyselinck. "Magnetic-equivalent-circuit modelling of switched reluctance machines with mutual coupling effects." Xxii International Conference on Electrical Machines IEEE, 2016

[2] Chen, Y., H. Liu, and J. Zhang. “Structure optimization and performance analysis of SRM with amorphous alloys core using FEM.” *Sensors & Transducers,* vol. 162, no. 1, pp. 273-279, 2014.

[3] Liang, De Liang, D. Wen, and Y. U. Zhen-Min. "Modeling for Switched Reluctance Motor Based on Adaptive Network-based Fuzzy Inference System." in *Proceedings of the Csee*, 2008.

[4] W.T. Pan, A new evolutionary computation approach: fruit fly optimization algorithm, in: *2011 Conference of Digital Technology and Innovation Management*, Taipei, 2011

[5] W.T. Pan, A new fruit fly optimization algorithm: taking the financial distress model, Knowl.-Based Syst. vol. 26, pp. 69-74, 2012.

[6] H. Li, S. Guo, C. Li, J. Sun, “A hybrid annual power load forecasting model based on generalized regression neural network with fruit fly optimization algorithm,” *Knowl.-Based Syst.* vol. 37, pp. 378 – 387, 2013 .

[7] S.M. Lin, “Analysis of service satisfaction in web auction logistics service using a combination of fruit fly optimization algorithm and general regression neural network,” *Neur. Comput. Appl.* vol. 7, pp.

459-465, 2013.

[8] J. Han, P. Wang, X. Yang, "Tuning of PID controller based on fruit fly optimization algorithm," in *proceeding of International Conference on Mechatronics and Automation (ICMA)*, pp. 409 – 413, 2012.

[9] P.W. Chen, W.Y. Lin, T.H. Huang, W.T. Pan,"Using fruit fly optimization algorithm optimized grey model neural network to perform satisfaction analysis for e-business service," *Appl. Math. Inf. Sci.*, vol. 7, pp. 459-465, 2013.

[10] X. Yuan, X. Dai, J. Zhao, et al. "On a novel multi-swarm fruit fly optimization algorithm and its application," *Appl. Math. Comput*. vol. 233, pp. 260 – 271, 2014.

[11] X. Yuan, X. Dai, J. Zhao, et al., "on a novel multi-swarm fruit fly optimization algorithm and its application", *Appl. Math. Comput*. vol. 233 pp. 260 – 271, 2014.

[12] L. Wang, Y. Shi, S. Liu, "An improved fruit fly optimization algorithm and its application to joint replenishment problems", *Expert Syst. Appl.* vol. 42, pp. 4310 – 4323, 2015.

[13] Specht, D. F. "A general regression neural network." *IEEE Trans Neural Networks* vol. 2, no. 6, pp.568-576, 1991.

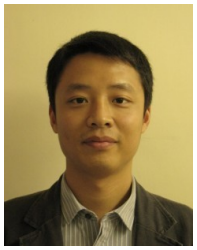

Zhu Zhang was born in Xiang Tan, Hunan Province, China in 1981. He received the B.S. degree in electrical engineering from Hunan Institute of Engineering in 2004, the M.S. degree in power electronics from the South China University of Technology in 2007 and the Ph.D. degree in electrical engineering from The Hong Kong Polytechnic University, Hong Kong, in 2012.

From 2007 to 2009, he was a Research Assistant with the Power Electronics Research Center, The Hong Kong Polytechnic University. From 2012 to 2013, he has been an Research Associate with the Electrical Engineering Department, The Hong Kong Polytechnic University. Since 2013, he has been a lecturer with College of Information and Electrical Engineering, Hunan University of Science and Technology. He is the author of more than 20 articles. His research interests include power electronics and power transmission, intelligent control etc.

Shenghua Rao was born in Wuhan, Hubei, china in 1993. He received his B. S. degree from Xiaoxiang College of Hunan University of Science and Technology in 2015. Form 2015，he is a master student in Hunan University of Science and Technology. His main research interests in power electronics and electrical driver system.

Xiaoping Zhang was born in Zhu Zhou, Hunan Province, China in 1966. He received the B.S. degree in automatic control from the Xi'an Jiao Tong University, Xi'an, in 1987 and the Ph.D. degree in mechanical and electronic engineering from the Central South University, Changsha, in 2008.

From 1987 to 1997, he was an engineer with the Technology Center, Xiangtan Electrical Machinery Group Co Ltd. From 1997 to 2000, he was an engineer with the Broad Air Conditioner Co Ltd. From 2000 to 2001, he was an engineer with the Technology Center, Zhuzhou Electric Locomotive Ltd. And from 2001 to 2010, he was a Professor with the Department of Electrical Engineering, Hunan University of Science and Technology. Since 2010, he has been a Professor with the National-Local Joint Engineering Laboratory of Marine Mineral Resources Exploration Equipment and Safety Technology, Hunan University of Science and Technology. He is the author of 25 computer software copyrights, more than 50 articles, holds eleven invention patents and 25 utility model patents. His research interests include power electronics and power transmission, intelligent control etc.